

# Single Molecule Magnetoresistance with Combined Antiferromagnetic and Ferromagnetic Electrodes

Alexei Bagrets,<sup>\*,†,‡</sup> Stefan Schmaus,<sup>§,||,■</sup> Ali Jaafar,<sup>⊥</sup> Detlef Kramczynski,<sup>§</sup> Toyo Kazu Yamada,<sup>§,¶</sup> Mébarek Alouani,<sup>⊥</sup> Wulf Wulfhekel,<sup>§,||</sup> and Ferdinand Evers<sup>†,■</sup>

<sup>†</sup>Institute of Nanotechnology and <sup>‡</sup>Steinbuch Centre for Computing, Karlsruhe Institute of Technology, Hermann-von-Helmholtz-Platz 1, 76344 Eggenstein-Leopoldshafen, Germany

<sup>§</sup>Physikalisches Institut and <sup>||</sup>DFG-Center for Functional Nanostructures, Karlsruhe Institute of Technology, Wolfgang-Gaede-Strasse 1, 76131 Karlsruhe, Germany

<sup>⊥</sup>Institut de Physique et Chimie des Matériaux de Strasbourg (IPCMS), UMR 7504 CNRS-ULP, 23 rue du Loess BP 43, 67034 Strasbourg, France

<sup>¶</sup>Graduate School of Advanced Integration Science, Chiba University, Chiba 263-8522, Japan

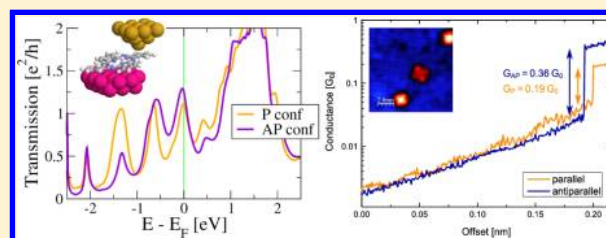
<sup>■</sup>Institut für Theorie der Kondensierten Materie, Karlsruhe Institute of Technology, Wolfgang-Gaede-Strasse 1, 76131 Karlsruhe, Germany

<sup>■</sup>Max-Planck-Institut für Festkörperforschung, Heisenbergstrasse 1, 70569 Stuttgart, Germany

## Supporting Information

**ABSTRACT:** The magnetoresistance of a hydrogen-phthalocyanine molecule placed on an antiferromagnetic Mn(001) surface and contacted by a ferromagnetic Fe electrode is investigated using density functional theory based transport calculations and low-temperature scanning tunneling microscopy. A large and negative magnetoresistance ratio of  $\sim 50\%$  is observed in combination with a high conductance. The effect originates from a lowest unoccupied molecular orbital (LUMO) doublet placed almost in resonance with the Fermi energy. As a consequence, irrespective of the mutual alignment of magnetizations, electron transport is always dominated by resonant transmission of Mn-majority charge carriers going through LUMO levels.

**KEYWORDS:** Spintronics, molecular electronics, nanomagnetism, giant magnetoresistance, phthalocyanine, antiferromagnetic Mn films



Modern information storage largely relies on basic spintronic devices such as the giant magnetoresistance (GMR) read heads.<sup>1,2</sup> These structures consist of two ferromagnetic layers separated by a nonmagnetic spacer. The conduction across the spacer in “current perpendicular to the plane” (CPP) GMR sensors depends on the relative orientation of the magnetization of the two ferromagnetic layers. To achieve high sensitivity for the magnetic stray fields of the recording medium, both a high change of the resistance and an easy modification of the relative magnetic orientation of the two layers by the external field are required. The latter is typically achieved by designing one of the layers to be soft magnetic and fixing the magnetization of the second layer by the exchange bias effect to an antiferromagnet.

A strong drive exists to downscale these magnetic sensors to the nanometer scale. Molecular electronics offers a pathway to achieve this aim by using single molecules as nonmagnetic spacer elements. Recently, it has been shown that a high GMR effect in combination with a low resistance can be achieved in electron transport across single hydrogen-phthalocyanine (H<sub>2</sub>Pc) molecules contacted with two ferromagnetic Co electrodes.<sup>3</sup> It has been found that even though the molecule

is nonmagnetic per se, the GMR can reach very large values,  $\sim 60\%$ . The effect has been understood as a consequence of spin-selective hybridization, being relevant also in the case of CoPc molecules adsorbed on ferromagnetic surfaces.<sup>4–6</sup> A very similar mechanism is active in magnetic films, including inorganic<sup>7,8</sup> and organic materials.<sup>9–11</sup>

A nanoscopic GMR junction with a single molecule as the nonmagnetic spacer offers the possibility to replace one of the ferromagnetic electrodes by an antiferromagnet. Because of the local nature of the contact to the antiferromagnetic electrode, the junction samples only the local magnetic order and a GMR can in principle be achieved. This structure has the advantage that the antiferromagnet is ideally hard magnetic, so that complex artificial antiferromagnets to pin the hard magnetic layer are not required.

Motivated by this idea, in this work we investigate a spin-selective hybridization of H<sub>2</sub>Pc to an antiferromagnetic

Received: May 24, 2012

Revised: August 13, 2012

Mn(001) surface with help of density functional theory (DFT) based transport simulations and low-temperature scanning tunneling microscopy (STM) measurements. In particular, we consider the Mn surface to be an interesting research object for two reasons. First, on the theoretical side, the work function of Mn ( $\approx 4.1$  eV) is below the Co one ( $\approx 5.0$  eV). This opens up a possibility to study resonant transport through the lowest unoccupied molecular orbital (LUMO) of H<sub>2</sub>Pc opposed to off-resonant transport found previously for the same molecules adsorbed at Co surface.<sup>3</sup> Second, on the experimental side, the antiferromagnetic order of the Mn thin films<sup>12</sup> allows, as mentioned above, for an alternative realization of a GMR device with only one ferromagnetic electrode.

**Single Resonant Level Model.** Charge and spin transport in molecular junctions are governed by electron transfer between the continuum of electronic levels in the electrodes and the molecular states. When a molecule is brought into contact to a metallic lead, first the molecular levels may shift in energy due to charge transfer to or from the molecule. Second, due to the coupling to the leads, the molecular states are broadened. A qualitative understanding of the spin selective broadening  $\Gamma_\sigma$  follows from the “golden rule” type expression<sup>13</sup>

$$\Gamma_\sigma(E) = |t_\sigma(E)|^2 \rho_\sigma(E)$$

Here,  $t_\sigma(E)$  denotes the coupling matrix element of a molecular orbital with a state of the substrate at energy  $E$ ;  $\sigma$  denotes the spin direction, and  $\rho_\sigma(E)$  is a spin-projected density of states in the substrate. Usually, one ignores the spin dependency in the coupling matrix,  $t_\sigma(E) \approx t(E)$ , so that

$$\Gamma_\sigma(E) \approx |t(E)|^2 \rho_\sigma(E)$$

The motivation behind is that the tunneling barrier separating the molecule from the substrate should exhibit only a weak dependency on the spin, because it is the interaction of the electrons inside the substrate, only, that discriminates spin directions. Hence,  $\Gamma_\sigma$  inherits its spin dependency predominantly from the surface magnetism that expresses itself as  $\rho_\uparrow(E_F) \neq \rho_\downarrow(E_F)$ .

The consequences for the magnetoresistance ratio<sup>14</sup>

$$\text{MR} = \frac{T_{\text{maj,maj}} + T_{\text{min,min}} - T_{\text{maj,min}} - T_{\text{min,maj}}}{T_{\text{maj,min}} + T_{\text{min,maj}}}$$

may be estimated for an isolated resonance at energy  $E_M$  with the Breit-Wigner expression for the transmission  $T(E_F)$

$$T_{S,D} = \frac{\Gamma^S \Gamma^D}{\Delta^2 + \frac{(\Gamma^S + \Gamma^D)^2}{4}} \quad (1)$$

where  $S, D = \{\text{maj}, \text{min}\}$  represent the spin states in the source (S) and drain (D) contacts,  $\Delta = E_M - E_F$ , and  $\Gamma^S$  and  $\Gamma^D$  to be evaluated at the Fermi energy,  $E_F$ . Here, we have assumed that the coupling of the molecule to the left and right leads, that is, substrate and STM tip, is symmetric, which implies  $\Gamma^{\text{maj}} = \Gamma_{\text{tip}}^{\text{maj}} = \Gamma_{\text{substr}}^{\text{maj}}$  and  $\Gamma^{\text{min}} = \Gamma_{\text{tip}}^{\text{min}} = \Gamma_{\text{substr}}^{\text{min}}$ .

In the off-resonant situation,  $\Delta \gg (\Gamma^S + \Gamma^D)$ , this simple model predicts a magnetoresistance ratio

$$\text{MR}^{\text{off}} = \frac{(1 - r_s)^2}{2r_s} \quad (2)$$

which is positive and controlled by a single parameter  $r_s = \Gamma^{\text{maj}} / \Gamma^{\text{min}}$ , the surface spin polarization. Details on the energetic

position of the resonance and the coupling matrix elements drop out in the magnetoresistance ratio, so that it is essentially insensitive to the exact energy of the resonance, that is, to the charge transfer between the molecule and the contacts. This case was relevant for explaining a recent experiment,<sup>3</sup> where the current was found to be carried by the LUMO with a displacement from the Fermi energy  $\Delta > (\Gamma^S + \Gamma^D)$ .

Let us now focus on the opposite case, that is, on resonant transport across a molecular level,  $\Delta \ll (\Gamma^S + \Gamma^D)$ . On the basis of the model formulated above, the on-resonance situation exhibits a magnetoresistance ratio,  $\text{MR}^{\text{on}} = \text{MR}^{\text{off}}/2$ . It is still positive, but  $\text{MR}^{\text{on}}$  is reduced as compared to the off-resonance case by a factor of 2. Our atomistic transport simulations presented below show that resonant transport is realized for H<sub>2</sub>Pc molecules adsorbed on the layer-wise antiferromagnet bct Mn(100) surface and contacted by an iron-coated STM tip. Furthermore, DFT calculations confirm (see Figure 1a) that in

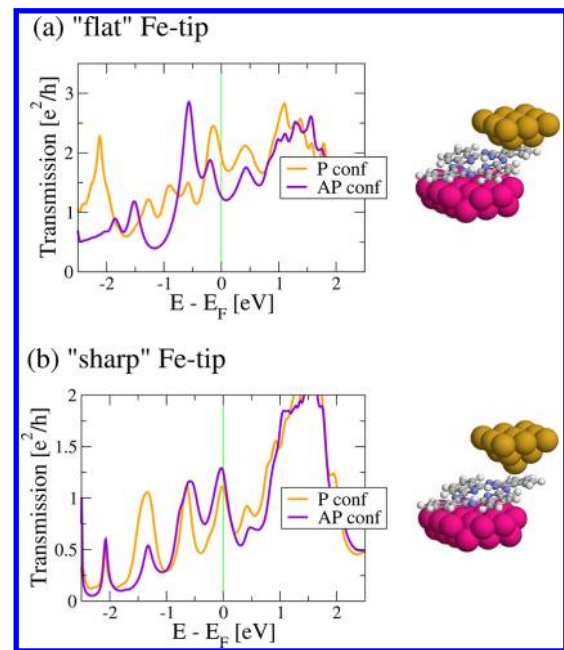


**Figure 1.** Model geometries of Mn(001)/H<sub>2</sub>Pc/Fe junctions and corresponding transmission curves computed assuming either parallel (P) or antiparallel (AP) alignment of magnetizations of the Mn (001) surface layer and the Fe tip. Atomic structures used for simulations are shown where the lower cluster models the Mn substrate, and the upper cluster the Fe tip. The molecule takes a slight bending when connecting the substrate with the tip. For computational details, see also Supporting Information. Upper plot (a): a geometry with the “flat” Fe tip exhibits a positive magnetoresistance ratio,  $\text{MR} = (T_P(E_F) - T_{AP}(E_F)) / T_{AP}(E_F)$ . Lower plot (b): in contrast, a geometry with the “sharp” Fe tip shows a reversed (negative) magnetoresistance ratio.

the case of Mn surface with a roughly symmetric coupling to the STM tip the GMR is indeed reduced, compared to the case of off-resonant transport. Namely, for our model geometry we have found a value  $\approx 50\%$ , which implies the surface spin polarization  $r_s \approx 0.27$  and which is smaller as compared to  $\text{GMR} \approx 65\%$  found earlier in the off-resonant case.<sup>3</sup>

Furthermore, the detailed DFT-studies suggest (see Figures 1a,b) that the magnetoresistance ratio is very sensitive to the atomistic details of the contact region. In the limit of a very weak coupling to the tunneling tip it can even change sign,

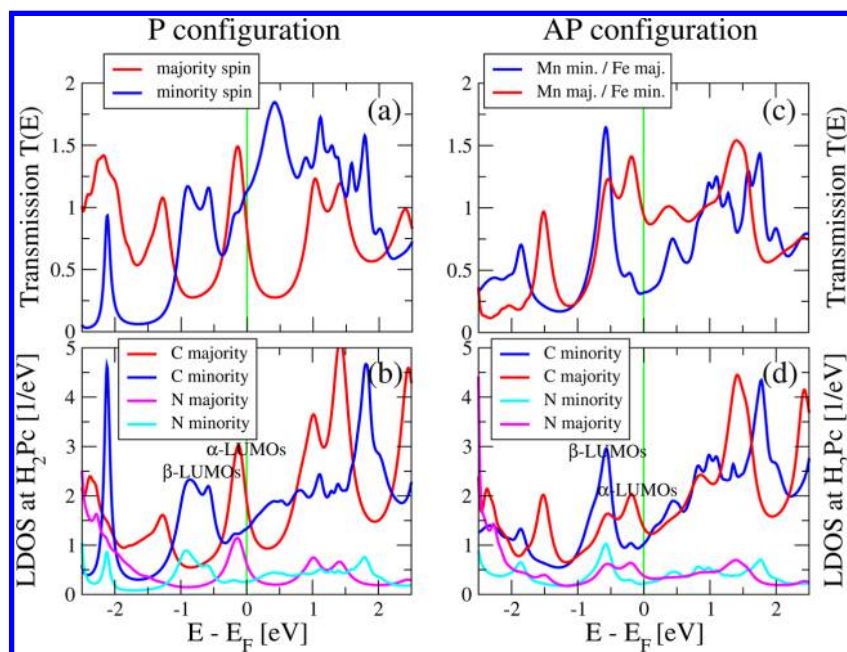


**Figure 2.** Electronic structure and transmission for “flat” tip geometry displayed in Figure 1a. Lower row (b,d): Local density of states in the  $H_2Pc$  molecule (projected to all carbon, upper traces; all nitrogen, lower traces). Majority spins ( $\alpha$ , red) and minority spins ( $\beta$ , blue). Upper row (a,c): Associated, spin-resolved transmission functions. Left column shows the case of parallel (P) alignment of magnetizations of the Fe tip and of the Mn (001) surface, right column shows antiparallel (AP) alignment. Plot highlights the fact that transmission resonances exhibit the spin-dependent hybridization. Near the Fermi energy there is a tendency for broad structures for minority spins and narrow lines for majority spins.

$MR^{on} < 0$ . A generalization of the simplified model to this case yields an estimate

$$MR^{on} = \frac{2}{r_a + \frac{1}{r_a}} - 1 \quad (3)$$

where now  $r_a = \Gamma_{\text{substr}}^{\text{maj}} / \Gamma_{\text{tip}}^{\text{min/maj}}$ . The assumptions are  $\Delta \approx 0$ ,  $\Gamma_{\text{tip}}^{\text{min/maj}} \ll \Gamma_{\text{substr}}^{\text{min/maj}}$ . Using an estimation  $r_a \approx 0.27$  for the surface spin polarization obtained for the case of symmetric coupling (see above), we get a negative magnetoresistance ratio,  $MR^{on} \approx -50\%$ . This numerical estimate is qualitatively consistent with the DFT-estimate  $MR^{on} \approx -15\%$  (see Figure 1b).

We show below that our experimental observations indeed confirm these theoretical estimates: the spread of the conductance data is substantially increased on Mn(001) as compared to the Co(111) surface (Figure 5), which we interpret as an indication of the enhanced contact sensitivity. Importantly, also the sign reversal of  $MR^{on}$  has been seen and the spread of measured values is well consistent with the theoretical limits.

**Adsorption Geometry.** To support our theoretical estimates based on the simplified resonant level model, we have performed accurate electronic structure and transport calculations for the  $H_2Pc$  molecules. The binding geometry of  $H_2Pc$  on the Mn/Fe(001) surface has been determined via standard slab calculations employing density functional theory within the local spin density approximation (LSDA), and gradient corrected approximation (GGA) amended by van der Waals (vdW) interactions within the Grimme scheme<sup>15</sup> (GGA+vdW). Details of calculations are given in the Supporting Information, Section I. In essence, symmetry considerations suggest to consider three binding geometries. In the “top” position two H atoms share the same Mn atom from the substrate, while in the “center” (or “hollow”) position they

share the same square surface facet. In the “bridge” position, two H atoms sit in neighboring facettes sharing the same link between two Mn atoms, see also Supporting Information Figure 2. For each one of these positions, we have determined the optimum distance between the molecule and the surface. We have found that when relaxing atoms within the LSDA, the “top” position was favored against the “center” one by 60 meV with an optimum distance of 2.1 Å. By contrast, the “bridge” position appeared to be discouraged with an additional energy cost of 3.1 eV. The GGA+vdW approach did not change the adsorption site but reduced slightly the adsorption distance to 1.93 Å.<sup>16</sup>

**Electronic Structure and Transmission.** The frontier states of  $H_2Pc$  are both ligand based with an associated highest occupied molecular orbital (HOMO)–LUMO gap of  $\sim 2.0$  eV (see Supporting Information, Section IIB). The HOMO is located on the outer organic shell with wave function nodes on the N atoms. By contrast, the LUMO is a doublet with wave function nodes located on six out of the eight N atoms. Because of the strong electronegative character of the nitrogen, the LUMO has a tendency to partially fill in the presence of a metal electrode. For this reason the LUMO of  $H_2Pc$  tends to be the current carrying orbital. This scenario has been found already for  $H_2Pc$  on Co(111)<sup>3</sup> and we expect it to be qualitatively valid as well for Mn surface.

For more quantitative estimates of charge transfer and level alignment we continue with our DFT-based analysis. Here, we consider two model geometries, with a “flat” (Figure 1a) and a “sharp” Fe tip (see Figure 1b), which account for the case of strong and weak coupling, respectively. We thus can investigate to what extent the contact details influence the electronic structure and hence also the transmission function.<sup>20</sup> More specifically, we assume that the molecule is slightly bent along the low-energy vibrational eigenmode ( $\omega \approx 15$  meV) when it is bound both to the substrate and to the STM tip. This choice

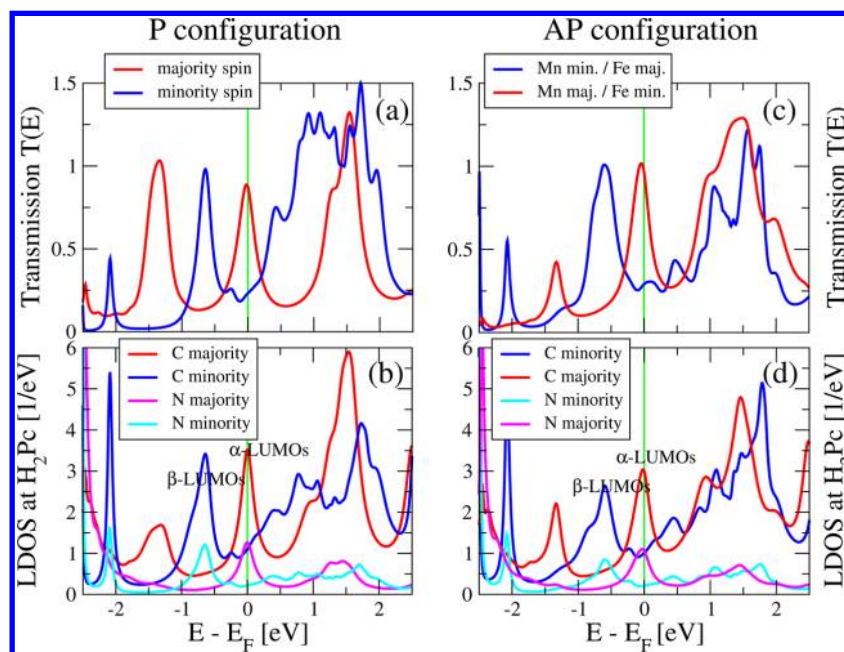


**Figure 3.** Figure analogous to previous one, Figure 2, now for the “sharp” tip geometry shown in Figure 1b.

was motivated by earlier STM experiments.<sup>3,22</sup> Furthermore, we suppose that  $d$  electrons of the low-coordinated Fe atoms can be involved in the covalent like bond with  $\pi$  electrons of a side phenyl ring of the molecule. A plausible binding mechanism, partly including also van der Waals interactions, is discussed in Section II of Supporting Information.

**Case of “Flat” STM Tip.** The results for the electronic structure of the “flat” tip geometry as encoded in the local density of states have been displayed in Figure 2. We first discuss the  $H_2Pc$ -projected (or local) density of state (LDOS) for the case of parallel (P) alignment of the spins in Fe tip and the Mn surface. As seen in Figure 2b, it exhibits the expected features. The majority spin resonance just below  $E_F$  represents the LUMO level partially filling with electrons supplied by the surrounding metal. Despite of the coupling, the resonance is very sharp due to the lack of available states for the majority spin carriers near  $E_F$  (for more information, see also Supporting Information, Figures 6 and 7). Moreover, spectral weight is found on N atoms and C atoms as well indicating the delocalized nature of the LUMO orbitals. By contrast, the minority LUMO state is shifted below  $E_F$  and has a significantly broader structure in the LDOS, which reflects the increased hybridization with the metal states. In the case of antiparallel (AP) alignment, there is no longer a clear distinction between minority and majority carriers any more, if the coupling to both electrodes is of a comparable strength. Indeed, as seen in Figure 2d, there is no well-developed distinction between the different spin channels, both exhibiting sharp LUMO resonances on broad background features (see also Supporting Information, Figure 7).

This situation readily carries over into the transmission functions, Figure 2a,c. We encounter a relatively pronounced LUMO resonance for parallel alignment in the majority channel, Figure 2a. By contrast, the minority transmission displays a strong broadening of the LUMO doublet that also produces significant transmission values above unity in a broad energy window. The associated transmissions add up to  $G^P = 1.94 e^2/h$  (Figure 1a). Again, nothing of this is seen in the

antiparallel configuration, Figure 2c. It exhibits two similar traces, both with peaked resonances on a broad background, irrespective of the spin direction;  $G^{AP} = 1.27 e^2/h$  (Figure 1a).

At this point our discussion shows that the “flat” tip configuration exhibits generic physics in the present on-resonance situation that is quite similar to the previously discussed system,  $H_2Pc$  on Co(111).<sup>3</sup> Consequently, one may expect that the simplified “toy” model could give a reasonable estimate for  $MR^{on}$ , which should be smaller (roughly, up to the one-half) than the value  $\approx 65\%$  found in ref 3. Our present estimate for the “flat” tip case supports this expectation, since the magnetoresistance ratio  $MR^{on} \approx 53\%$  is reduced by magnitude.

**Case of “Sharp” STM Tip.** The characteristic feature of the “flat” configuration was the (roughly) symmetric way in which both electrodes couple to the molecule. We now investigate the opposite situation where the tip is atomically sharp, see Figure 1b. In this case, the coupling of the molecule to the STM tip is significantly weaker than the one to the substrate. Hence the line width of all resonances and also the level filling is largely determined by the substrate.

As a consequence one can formulate the following expectations for the asymmetric case: the typical line width is reduced as compared to the symmetric coupling and there is a certain shift of the DFT-LUMO due to a slightly modified charge transfer. Moreover, in the case of antiparallel alignment of magnetizations, traces for up-spin and down-spin electrons should be significantly different, since reversing majority and minority spins in substrate and tip no longer is an (approximate) symmetry operation (see also Supporting Information Figure 8).

As may be inferred from Figure 3, the simulation data confirm all these expectations. In particular, they display a LUMO transport resonance for the majority channel that is very sharp and located at  $E_F$ . For this reason, transport is completely dominated by majority spin carriers, which is in pronounced contrast to the symmetric, “flat” Fe tip case. The second important difference relates to the conductances. We

read off  $G^P \approx 1.1 e^2/h$  and  $G^{AP} \approx 1.25 e^2/h$  (see Figure 1b), so the value for the antiparallel alignment of magnetizations in the contacts does exceed the parallel one. Correspondingly, the GMR is negative,  $MR^{on} \approx -13\%$ . While the sign may be understood within the simplified model already, the magnitude of the effect is not predicted. This is because the “toy” model is valid in the limit of an extremely asymmetric coupling, in which all transmission peaks have values significantly below unity. The DFT-model calculation is not fully in this limit, yet, as the DFT-conductances are still quite large. Furthermore, in DFT-simulation the precise value of the negative GMR ratio is sensitive to the centering of the narrow majority spin LUMO resonance about  $E_F$ .<sup>21</sup>

**STM Experiments.** To support our theoretical findings, we have performed as the second step electron transport measurements with the scanning tunneling microscope. Spin-polarized conductance versus distance curves<sup>3,22</sup> have been measured on top of  $H_2Pc$  molecules adsorbed on an antiferromagnetic Mn surface. The surface was prepared by evaporating a few layers of Mn (6–8 ML) on the clean Fe(001) surface of an home-grown Fe whisker. Depending on the exact number of Mn layers different magnetic domains are formed<sup>24,25</sup> (see Figure 4b). For obtaining spin resolution, a

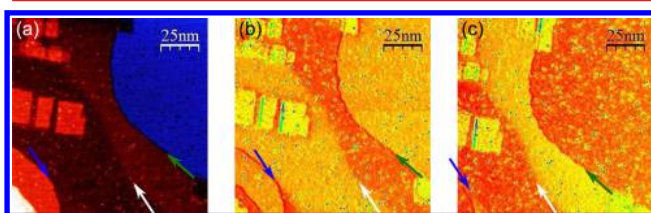


**Figure 4.** (a) Topographical image of Mn grown on an Fe(001) whisker. (b)  $dI/dV$  map taken before reversing the external field. (c)  $dI/dV$  map after reversing the external field. The three arrows indicate the main magnetic features of the Mn/Fe(001) surface. Green: a Mn step edge at the surface, that is visible in the topography and the  $dI/dV$  maps. White: a buried Fe step edge, that is only slightly visible in the topography but can clearly be seen in the  $dI/dV$  map. Blue: coincident Fe and Mn step edges. The magnetic effect is compensated ( $V = 200$  mV,  $T = 4.3$  K).

wet etched W tip has been coated with a thin Fe film resulting in an in-plane magnetized tip. By measuring spatial resolved ( $dI/dV$ ) maps at 200 mV the domains could be identified. By applying a small external field the relative orientation of the tip and substrate magnetizations could be reversed. This has been evidenced by the reversed spin contrast (see Figure 4c).

After magnetic contrast has been achieved, conductance versus distance curves have been recorded on molecules in dependence of the mutual orientation of tip and surface magnetizations. In Figure 5, a representative example of conductance versus distance curves for the two magnetic configurations (P versus AP) is shown. When the tip is approaching the  $H_2Pc$  molecule, a characteristic jump in the conductance is observed, which is attributed to the formation of a molecular junction driven by the excitation of a soft vibrational mode of the molecule.<sup>22</sup> After the molecular junction is formed, its conductance strongly depends on the mutual alignment of magnetizations in the electrodes. While the conductance in the tunneling regime is higher for the parallel as compared to the antiparallel alignment, the reversed situation is observed in the “contact” regime. In order to make a reliable estimate for the GMR value, the measurements have been repeated several hundred times for both mutual alignments of magnetizations. Figure 5b shows the distribution of the conductance values obtained in the 161 transport experiments. On average, the spin dependent molecular conductances have been estimated as  $G^P = (0.286 \pm 0.013) G_0$  and  $G^{AP} = (0.441 \pm 0.026) G_0$ , where  $G_0 = 2e^2/h$  is the conductance quantum. This results in the negative MR ratio for the Mn/ $H_2Pc$ /Fe junction, namely  $GMR = (G^P - G^{AP})/G^P = -(54 \pm 16)\%$ . While the absolute value of GMR is close to that one measured previously on  $H_2Pc$  in between the two Co electrodes, the sign of the MR ratio is negative. This negative MR ratio correlates with a prediction of the DFT-based simulations for the atomically “sharp” tip geometry. We note, however, that the strong spread in measured conductances observed in current experiment indicates the strong influence of different contact geometries on the on-resonance electron transmission. While similar variations of the conductance have been found in nonmagnetic transport measurements,<sup>26</sup> our results indicate that this effect persists also in case of spin-

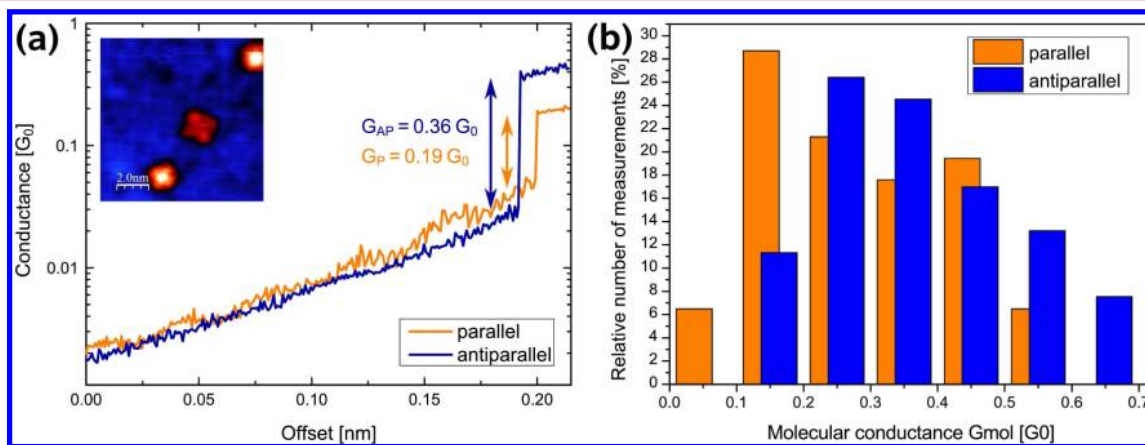


**Figure 5.** (a) Exemplary conductance versus distance curves measured across  $H_2Pc$  on Mn/Fe(001). The jump height in the antiparallel (AP) case is much higher than in the parallel (P) case. This results in the large and negative GMR ratio. Inset plot is a topographical STM image of  $H_2Pc$  molecules adsorbed on Mn/Fe(001). (b) Distribution of the conductance values, measured for the P and AP configurations, obtained in the 161 transport experiments.

dependent transport across a single molecule in the ballistic regime.

To summarize, we have investigated the magnetoresistance of an H<sub>2</sub>Pc molecule adsorbed on an Mn(001) substrate by means of DFT-based simulations and low-temperature STM measurements employing an Fe tip. A theoretical analysis shows that due to spin-dependent hybridization of the molecule's and electrodes' electronic states, a nonmagnetic molecule can exhibit a strong GMR effect even when one of the electrodes is an antiferromagnet, which is confirmed by our experimental data. Interestingly, a negative GMR value was observed, which has been explained on the basis of a resonant transport across the LUMO level of the molecule in combination with asymmetric coupling of the H<sub>2</sub>Pc with magnetic electrodes.

## ■ ASSOCIATED CONTENT

### 📄 Supporting Information

Additional figures and information. This material is available free of charge via the Internet at <http://pubs.acs.org>.

## ■ AUTHOR INFORMATION

### Corresponding Author

\*E-mail: Alexej.Bagrets@kit.edu.

### Notes

The authors declare no competing financial interest.

## ■ ACKNOWLEDGMENTS

We thank M. Bowen and E. Beaupaire for discussions on the molecule–metal interface and J. Arabski for purifying the molecules. T.K.Y. acknowledges funding by the Alexander-von-Humboldt foundation. A.B., S.S., F.E., and W.W. acknowledge funding by the DFG (Deutsche Forschungsgemeinschaft), the Center for Functional Nanostructures (CFN) and the Baden-Württemberg Stiftung.

## ■ REFERENCES

- (1) Baibich, M. N.; Broto, J. M.; Fert, A.; Van Dau, F. N.; Petroff, F.; Etienne, P.; Creuzet, G.; Friederich, A.; Chazelas, J. *Phys. Rev. Lett.* **1988**, *61*, 2472–2475.
- (2) Binasch, G.; Grünberg, P.; Saurenbach, F.; Zinn, W. *Phys. Rev. B* **1989**, *39*, 4828–4830.
- (3) Schmaus, S.; Bagrets, A.; Nahas, Y.; Yamada, T. K.; Bork, A.; Bowen, M.; Beaupaire, E.; Evers, F.; Wulfhchel, W. *Nat. Nanotechnol.* **2011**, *6*, 185–189.
- (4) Iacovita, C.; Rastei, M. V.; Heinrich, B. W.; Brumme, T.; Kortus, J.; Limot, L.; Bucher, J. P. *Phys. Rev. Lett.* **2008**, *101*, 116602.
- (5) Atodiresei, N.; Brede, J.; Lazić, P.; Caciuc, V.; Hoffmann, G.; Wiesendanger, R.; Blügel, S. *Phys. Rev. Lett.* **2010**, *105*, 066601.
- (6) Brede, J.; Atodiresei, N.; Kuck, S.; Lazić, P.; Caciuc, V.; Morikawa, Y.; Hoffmann, G.; Blügel, S.; Wiesendanger, R. *Phys. Rev. Lett.* **2010**, *105*, 047204.
- (7) Bowen, M.; et al. *J. Phys.: Condens. Matter* **2007**, *19*, 315208.
- (8) Greullet, F.; Tiusan, C.; Moutagne, F.; Hehn, M.; Halley, D.; Bengone, O.; Bowen, M.; Weber, W. *Phys. Rev. Lett.* **2007**, *99*, 187202.
- (9) Santos, T. S.; Lee, J. S.; Migdal, P.; Lekshmi, I. C.; Satpati, B.; Moodera, J. S. *Phys. Rev. Lett.* **2007**, *98*, 016601.
- (10) Barraud, C.; Seneor, P.; Mattana, R.; Fusil, S.; Bouzehouane, K.; Deranlot, C.; Graziosi, P.; Hueso, L.; Bergenti, I.; Dediu, V.; Petroff, F.; Fert, A. *Nat. Phys.* **2010**, *6*, 615–620.
- (11) Javald, S.; Bowen, M.; Boukari, S.; Joly, L.; Beaufrand, J.-B.; Chen, X.; Dappe, Y. J.; Scheurer, F.; Kappler, J.-P.; Arabski, J.; Wulfhchel, W.; Alouani, M.; Beaupaire, E. *Phys. Rev. Lett.* **2010**, *105*, 077201.
- (12) Wulfhchel, W.; Schlickum, U.; Kirschner, J. *Microsc. Res. Tech.* **2005**, *66*, 106–116.
- (13) Bruus, H.; Flensberg, K. *Many-body quantum theory in condensed matter physics: an introduction*; Oxford University Press: New York, 2004.
- (14) We define the magnetoresistance ratio as  $MR = (G^P - G^{AP})/G^{AP}$ , where  $G^P$  and  $G^{AP}$  are conductances across molecular junctions with electrodes being magnetized either parallel (P) or antiparallel (AP) to each other.
- (15) Grimme, S. *J. Comput. Chem.* **2006**, *27*, 1787–1799.
- (16) It is interesting to mention that binding geometries are not very sensitive to whether the LSDA or the GGA+vdW have been used. This seems surprising, however, it is well-known that LSDA has a tendency to overestimate and GGA to underestimate the binding energies. For example, LDA reproduces the distance between graphite layers<sup>17</sup> whereas GGA gives correct results only when the vdW interactions are included.<sup>18</sup> A similar situation was also found for the adsorption of CoPc on Co(111) surface.<sup>19</sup>
- (17) Spanu, L.; Sorella, S.; Galli, G. *Phys. Rev. Lett.* **2009**, *103*, 196401.
- (18) Rydberg, H.; Dion, M.; Jacobson, N.; Schröder, E.; Hyldgaard, P.; Simak, S. I.; Langreth, D. C.; Lundqvist, B. I. *Phys. Rev. Lett.* **2003**, *91*, 126402.
- (19) Chen, X.; Alouani, M. *Phys. Rev. B* **2010**, *82*, 094443.
- (20) Probably, none of the model geometries displayed in Figure 1 is particularly close to the experimental situation, for example, due to the presence of strain. Still, important insights will be gained about the molecular conductance since qualitative features, like contact sensitivity, and also quantitative information, like the spread in magnetoresistance values, will be properly reproduced by our modeling.
- (21) We emphasize that the alignment of molecular levels with the Fermi energy of the metal electrodes suffers from approximations in the exchange-correlation functionals that one employs in DFT calculations.<sup>23</sup> Usually, DFT properly reproduces trends but not necessarily the precise resonance position. Therefore, quantitative deviations of the position of the true LUMO resonance from the values that one reads off Figures 1 and 2 are to be expected. However, as has already been pointed out in ref 3 the GMR is a ratio of two conductances and therefore a tendency for error cancellation exists. Hence, we believe that our estimates for the GMR could be quantitatively more robust against functional artifacts than the transmission function itself.
- (22) Takács, A. F.; Witt, F.; Schmaus, S.; Balashov, T.; Bowen, M.; Beaupaire, E.; Wulfhchel, W. *Phys. Rev. B* **2008**, *78*, 233404.
- (23) Evers, F.; Burke, K. Pride, prejudice, and penury of ab initio transport calculations for single molecules. In *Nano and Molecular Electronics Handbook*; Lyshevski, S. E., Ed.; CRC Press: Boca Raton, FL, 2007.
- (24) Yamada, T. K.; Bischoff, M. M. J.; Heijnen, G. M. M.; Mizoguchi, T.; van Kempen, H. *Phys. Rev. Lett.* **2003**, *90*, 056803.
- (25) Schlickum, U.; Janke-Gilman, N.; Wulfhchel, W.; Kirschner, J. *Phys. Rev. Lett.* **2004**, *92*, 107203.
- (26) Schull, G.; Frederiksen, T.; Arnau, A.; Sanchez-Portal, D.; Berndt, R. *Nat. Nanotechnol.* **2011**, *6*, 23–27.